Missense Mutations in the Sodium Borate Cotransporter SLC4A11 Cause Late-Onset Fuchs Corneal Dystrophy

ARTICLE *in* HUMAN MUTATION · NOVEMBER 2010

Impact Factor: 5.14 · DOI: 10.1002/humu.21356 · Source: PubMed

12 AUTHORS, INCLUDING:

Danielle N Meadows
McGill University
8 PUBLICATIONS **189** CITATIONS
SEE PROFILE

Allen O Eghrari
Johns Hopkins Medicine
24 PUBLICATIONS **317** CITATIONS
SEE PROFILE

John D Gottsch
Johns Hopkins Medicine
49 PUBLICATIONS **1,297** CITATIONS
SEE PROFILE

Published in final edited form as:
Hum Mutat. 2010 November ; 31(11): 1261–1268. doi:10.1002/humu.21356.

Missense mutations in the sodium borate co-transporter *SLC4A11* cause late onset Fuchs corneal dystrophy

S. Amer Riazuddin[1,2], **Eranga N. Vithana**[3,4], **Li-Fong Seet**[3], **Yangjian Liu**[1], **Amr Al-Saif**[1], **Li Wei Koh**[3], **Yee Meng Heng**[5], **Tin Aung**[3], **Danielle N. Meadows**[2], **Allen O. Eghrari**[2], **John D. Gottsch**[2], and **Nicholas Katsanis**[1,6]

[1] McKusick-Nathans Institute of Genetic Medicine, Johns Hopkins University School of Medicine, Baltimore MD 21205

[2] The Wilmer Eye Institute, Johns Hopkins University School of Medicine, Baltimore MD 21287

[3] Singapore Eye Research Institute, 11 Third Hospital Avenue, Singapore 168751

[4] Department of Ophthalmology, Yong Loo Lin School of Medicine, National University of Singapore

[5] Institute of Medical Biology, A*STAR, Singapore 117597

[6] Center for Human Disease Modeling, Departments of Cell Biology and Pediatrics, Duke University Durham NC 27710

Abstract

Homozygous mutations in the sodium-bicarbonate transporter *SLC4A11* cause two early onset corneal dystrophies: congenital hereditary endothelial dystrophy (CHED) and Harboyan syndrome. More recently, four sporadic patients with late onset Fuchs corneal dystrophy (FCD), a common age-related disorder, were also reported to harbor heterozygous mutations at this locus. We therefore tested the hypothesis that *SLC4A11* contributes to FCD and asked whether mutations in *SLC4A11* are responsible for familial cases of late onset FCD. We sequenced *SLC4A11* in 192 sporadic and small nuclear late-onset FCD families and found seven heterozygous missense novel variations that were absent from ethnically matched controls. Familial data available for one of these mutations showed segregation under a dominant model in a three-generational family. *In silico* analyses suggested that most of these substitutions are intolerant, while biochemical studies of the mutant protein indicated that these alleles impact the localization and/or post-translational modification of the protein. These results suggest that heterozygous in *SLC4A11* are modest contributors to the pathogenesis of adult FCD, suggesting a causality continuum between FCD and CHED. Taken together with a recent model between FCD and yet another early onset corneal dystrophy, PPCD, our data suggest a shared pathomechanism and genetic overlap across several corneal dystrophies.

Keywords

SLC4A11; Fuchs corneal dystrophy; anterior segment; corneal endothelium

Correspondence to: Nicholas Katsanis, katsanis@cellbio.duke.edu, tel: 1-919 613 4694; fax 1-919 684 1627.

Introduction

Corneal endothelial dystrophies are a group of clinically and genetically heterogeneous disorders characterized by abnormalities of the corneal endothelium and Descemet membrane (Klintworth, 2009). Traditional clinical compartmentalization based on unique features has recognized four major early-onset corneal endothelial dystrophies: Congenital hereditary endothelial corneal dystrophy (CHED), X-linked endothelial corneal dystrophy (XECD), early-onset Fuchs endothelial corneal dystrophy (FECD), and posterior polymorphous corneal dystrophy (PPCD. Although clinically distinct, most of them manifest a defective fluid transport by the corneal endothelium, which causes excessive edema of the corneal stroma and this impairs the clarity of the cornea and reduces visual acuity (Klintworth, 2009).

At the other end of the spectrum, late-onset Fuchs corneal dystrophy (FCD) is recognized as the most common inherited corneal dystrophy; first described in the early 20th century, adult onset FCD is characterized by the formation of guttae, microscopic protrusions of the basal lamina that underlies the corneal endothelium. Generally, the disease onset begins in the fifth decade of life, is more common among women (Fuchs, 1910; Vogt, 1921) and progresses slowly over the next two to three decades (Krachmer et al., 1978). FCD initiates with deterioration of endothelial cell borders and loss of cell density, resulting in decreased overall endothelial cell pump function (Vincent et al., 2003). Failure to pump water out of the stroma results in corneal edema, which leads to visual impairment. The end-stage of the disease is characterized by degeneration of the corneal endothelium with the consequent failure of its ion transport and solute barrier functions (Hogan et al., 1974; Wilson and Bourne, 1988).

Traditional positional cloning approaches have provided some clues as to the pathology of the endothelial corneal dystrophies, although a unifying paradigm(s) remains elusive. Nonsense mutations in *TCF8* (MIM# 189909) have been identified in PPCD patients (Krafchak et al., 2005; Aldave et al., 2007), whereas homozygous missense and nonsense mutations in *SLC4A11* (MIM# 610206) have been implicated in CHED (Vithana et al., 2006). Similarly, mutations in *VSX1* (MIM# 605020) has been associated with PPCD and keratoconus (Heon et al., 2002; Bisceglia et al., 2005), however this result is yet to be replicated. With regard to FCD, the early-onset form is attributed to defects in *COL8A2* by virtue of the presence p.L450W and p.Q455L point mutations (Biswas et al., 2001; Gottsch et al., 2005).

Late-onset form of FCD is an autosomal dominant disorder manifesting incomplete penetrance, variable expressivity and a high phenocopy rate. Nonetheless, four late-onset FCD loci have now been mapped *FCD1*, *FCD2*, *FCD3*, and *FCD4* on chromosomes 13, 18, 5 and 9, respectively,(Sundin et al., 2006b; Sundin et al., 2006a; Riazuddin et al., 2009; Riazuddin et al., 2010) with the *FCD2* locus likely contributing >30% of the mutational load. Interestingly, screening of a cohort of 86 sporadic FCD individuals of Chinese and Indian decent for *SLC4A11* uncovered four likely loss of function mutations, raising the possibility of a genetic overlap between the endothelial corneal dystrophies (Vithana et al., 2008). In support of that model, we showed recently that loss-of-function mutations in *TCF8* are sufficient to cause adult-onset FCD and can interact with *FCD4* to modulate the severity of the disorder (Riazuddin et al., 2010). We therefore focused our attention to *SLC4A11* and interrogated our entire cohort of sporadic and familial cases for evidence of involvement in late-onset FCD.

Material and Methods

Patient Ascertainment

We ascertained a cohort of 192 sporadic cases and members of small nuclear FCD families. All patients underwent detailed ophthalmic evaluation that included slit lamp biomicroscopy performed at the Wilmer Eye Institute. Affectation status and disease severity were determined with the scale proposed by Krachmer and colleagues (Krachmer et al., 1978). Positive disease status was indicated if the patient had a minimum Fuchs Krachmer grading score of 1, which represented 12 or more central non-confluent guttae, in at least one eye. The study protocol was approved by the Joint Committee on Clinical Investigation at the Johns Hopkins University School of Medicine, and is in accordance with the Declaration of Helsinki. Informed written consent was obtained from all study participants and the study is in accordance with HIPAA regulations. Approximately 10 ml blood was collected from each study participant. DNA was extracted using Gentra Puregene Blood Kit (Qiagen, Santa Clara, CA).

Mutation Screening

Individual exons of *SLC4A11* and *VSX1* were amplified by PCR using primer (primer sequences and annealing temperatures are available upon request). Amplifications were performed in 25ul reactions containing 30ng of genomic DNA, 2.5 μl 10X PCR Buffer, 2.5 μl 2 mM dNTPs, 2.5 μl of 5M Betaine, 10 pmoles of each primer, and 0.2 U *Taq* DNA polymerase. Unincorporated primers and dNTPs were removed by treating the PCR product with an exonuclease (Exonucleae1) and Shrimp alkaline phosphate according to manufacturer's instructions (USB Cleveland OH). The PCR primers for each exon were used for bidirectional sequencing using Big Dye Terminator Ready reaction mix according to manufacturer instructions (Applied Biosystems). Sequencing was performed on an ABI PRISM 3100 Automated sequencer (Applied Biosystems). Sequencing results were assembled and analyzed with Sequencher. The sequence variants identified in SLC4A11 were designated based on cDNA sequence with +1 corresponding to the A of the ATG translation initiation codon in the GenBank reference sequence: NM_032034.3).

Prediction Analysis

The degree of evolutionary conservation of positions at which missense mutations exist and the possible impact of an amino acid substitution on the structure of SLC4A11 protein were examined with the SIFT and PolyPhen algorithms. Evolutionary conservation of the mutated amino acids was examined using the USCS genome browser. The SLC4A11 domain structure was predicted with Simple Modular Architecture Research Tool (SMART) software.

Generation of site directed mutants

Cloning of *SLC4A11* cDNA for *in vitro* experiments has been described previously (Vithana et al., 2006). Single point mutations identified in our cohort were introduced into human *SLC4A11* cloned in phCMV2 vector (Gene Therapy Systems, San Diego CA) using site-directed mutagenesis Kit according to manufacturer's instructions (Stratagene, La Jolla, CA). The presence of each mutation was confirmed with bidirectional sequencing. Additionally, the entire *SLC4A11* ORF for each clone was sequenced to rule out the presence of other mutations that may have been incorporated during the mutagenesis procedure.

Immunoblot analysis of protein extracts

WT SLC4A11 and mutant variants of SLC4A11 were expressed as HA-tagged proteins by transient transfection of HEK293T cells with 2 μg of the indicated vector constructs using Lipofectamine2000 (Invitrogen Corp). Cells were grown at 37 °C in 5% CO_2 in Dulbecco's modified Eagle media (DMEM) supplemented with 10% (v/v) fetal bovine serum (Gibco-Invitrogen Corporation, Burlington, ON, Canada). Cells were lysed in lysis buffer containing 20 mM Tris-buffer, pH 7.4, 150 mM NaCl, 1 mM EDTA, 0.5% (v/v) Triton X-100, 2 mM $MgCl_2$, 1 mM DTT and Complete Protease Inhibitor Cocktail Tablets (Roche Applied Science, Mannheim, Germany). Protein quantification was done using Commassie Plus (Thermo Fisher Scientific Inc., IL, USA). Samples were heated to 65°C for 5 min before being resolved by SDS-PAGE and transferred to PVDF membranes (Bio-Rad Laboratories, Hercules, CA, USA) for immunodetection. Overexpressed HA-tagged SLC4A11 proteins were detected using a monoclonal anti-HA antibody (16B12, Covance, Richmond, CA, USA) followed by a rabbit anti-mouse IgG conjugated to horseradish peroxidase (ZYMED, USA) and visualized using the SuperSignal West Femto Maximum Sensitivity Substrate (Thermo Fisher Scientific Inc., IL, USA). Intensities of the detected protein species were quantified by densitometry using the Station 440CF (Carestream Molecular Imaging., New Haven, USA).

Enzymatic Deglycosylation

HEK293 cells were transfected and lysed as described above. Enzymatic deglycosylation was performed as described previously.(Vithana et al., 2008) Briefly, two days post-transfection, cells were washed with PBS and solubilized by addition of 1 ml of IPB buffer supplemented with protease inhibitors (Mini Complete, Roche Molecular Biochemical). The Bradford assay was used to assess the amount of protein in the cell lysates. Lysate samples (10 μg of protein) were heated 5 min at 65 °C and then incubated with 5 μl (2500 units) of N-glycosidase F (PNGase F) or3 μl of Endo H (1500 units) (New England Biolabs) for 2 h at 37°C. Reactions were stopped by the addition of 2xSDS PAGE sample buffer. Samples were electrophoresed on5% acrylamide Tricine gels. Immunoblots were transferred to PVDF membranes and probed with an anti-HA antibody 1:2000(16B12, Covance Richmond, USA).

Confocal immunolocalization

HEK293T cells grown on coverslips were transiently transfected as described above, and were then fixed with 4 % (w/v) paraformaldehyde and permeabilized with 0.1% (v/v) Triton X-100 in PBS. Cellular distribution of each overexpressed HA-tagged SLC4A11 protein was visualized by incubating the cells with rabbit polyclonal anti-HA antibody (Y-11, SC 805 Santa Cruz Biotechnology, CA, USA) followed by goat anti-rabbit IgG conjugated with AlexaFluor 594 (Invitrogen Corp). DNA was visualized by co-incubating the cells with diamidino-2-phenylindole (DAPI) purchased from Sigma Inc.. Cells were imaged with a Zeiss LSM510 confocal microscope (Zeiss, USA).

Results

Screening late-onset FCD patients for pathogenic mutations in *SLC4A11*

Given the recent involvement of *TCF8* in the pathogenesis of late-onset FCD (Riazuddin et al., 2010) and the finding of four likely deleterious point mutations in *SLC4A11* in another adult-onset FCD cohort (Vithana et al., 2008), we pursued the hypothesis that genes implicated in both dominant and recessive early-onset corneal dystrophies could have a contributory role to the development of the late-onset forms of the disease. We therefore

screened all coding sequences and intron-exon junctions of both *SLC4A11* and *VSX1* in a cohort of 192 FCD patients, composed of both sporadic and familial cases.

To avoid potential problems with ethnic-specific alleles that might not be well matched with our controls, we focused on patients of northern European decent, all of whom exhibited typical characteristics of FCD. The first symptoms of disease appeared in their early forties, progressive corneal guttae formation bilaterally. Individuals with Krachmer grading score of 1 or above were considered affected whereas individuals with less than 12 guttae or unilateral findings (age >65) were considered negative or unaffected. With the exception of two HapMap SNPs, we found no evidence for pathogenic mutations in *VSX1*. By contrast, we found seven missense mutations in *SLC4A11* that were absent from both 192 control chromosomes and from HapMap (Table 1). These seven alleles encode amino acid substitutions (p. E167D, p.R282P, p.Y526C, p.V575M, p.G583D, p.G742R and p.G834S;) that map to functional domains within SLC4A11, with 5/7 alleles clustering in the bicarbonate domain and four of the alleles residing within one of the 12 transmembrane domains (Fig. 1).

Evolutionary analysis showed the E167, R282, G583, G742 positions to be invariant across all species with a detectable SLC4A11 ortholog (best reciprocal BLAST hit), while two positions, V575 and G834 were conserved across mammals; the Y526 site was the only poorly conserved position. Consistent with these observations, both SIFT and PolyPhen predicted 5/7 to be pathogenic (E167D and Y526C were predicted to be benign).

To interrogate further the possible role of these alleles to the development of FCD, we revisited the probands bearing each of the seven mutations. In one instance, we were able to expand and recruit three affected and two unaffected individuals from a proband with the G742R mutation, deemed pathogenic by all other criteria. Subsequent to confirming the disease phenotype (or absence thereof) with slit-lamp and retro-illumination photography, we found the candidate disease allele to segregate in a dominant fashion (Fig. 2). Notably, although individual -08 was too young to consider for formal diagnosis, our analysis predicted genotypically that she would be affected and we did detect the presence of central guttae, suggestive of early disease.

Examining the Stability, Processing and Post-translational modifications of SLC4A11 mutants

We next sought to obtain more direct evidence for the possible effect of the seven *SLC4A11* alleles. Previous work has suggested that some of the mutations found in adult onset FCD patients might interfere with either the stability and processing of the protein, its glycosylation, or its final insertion in the plasma membrane (Vithana et al., 2008). We therefore expressed HA-tagged wild type (wt) SLC4A11 as well as constructs bearing each of the seven mutations in HEK293T cells and examined each of the three aspects of the proteins production and functionalization. Consistent with previous findings, we observed immunoblotted wt SLC4A11 to migrate as two protein species of approximately 120 kDa and 80 kDa respectively, corresponding to mature and immature forms of SLC4A11 (Vithana et al., 2008). Analysis of each of the seven mutants in triplicate experiments showed that although four of them (p.V575M, p.G742R, p.E167D and p.G834S) were processed in a manner indistinguishable from wt, the other three showed marked differences in processing (Fig. 3A, B, C). Specifically, The p.R282P mutant expressed the immature form as the predominant form, with significantly less contribution to the mature 120kDa species ($p<0.005$); in addition, the amount of mature protein was likewise reduced significantly compared to wt ($p<0.005$), suggesting degradation, possibly triggered by misfolding. We observed a significant ($p<0.005$) reduction in both the 80 kDa and of 120 kDa species for the G583D mutant, likewise suggesting proteolytic degradation. Moreover,

the p.E167D and p.G742R mutant proteins showed an additional band of approximately 100kDa and also had less contribution to the mature 120kDa protein specie (Fig. 3C). This 100kDa band was also observed in the WT SLC4A11, but to a much less degree, when protein extracts were subjected to higher resolution by 5% SDS-PAGE, and probably represents a post-ER glycosylated form of SLC4A11. However the E167D and G742R mutant proteins did not induce any significant decrease in the level of protein expression; rather, they showed a reduction in the processing to the mature 120kDa form (Fig. 3C), suggesting that they are not as grossly unfolded as others to be highly susceptible to proteolytic degradation but is in a non-native conformation resulting in inefficient processing to the plasma membrane.

We next turned to the question of post-translational modification. Previous work has demonstrated that the 120 kDa form of SLC4A11 represents complex glycosylation, associated with cellular locations postER, while the 80 kDa form, shiftable to the position below 80 kDa upon endoglycosidase-H (Endo H) treatment, represents the core-glycosylated protein found in the ER.(Vithana et al., 2008) The form below 80 kDa represents protein devoid of N-linked glycosylation. These three bands thus serve as markers for mature (complex) glycosylated, core glycosylated, and unglycosylated forms of SLC4A11 (Fig. 3D). We observed no significant differences in de-glycosylation patterns compared with wt, indicating that glycosylation is not grossly affected by these lesions. However, we did observe (on high resolution SDS-PAGE) a persistent ~100kDa species in the p.G742R and p.E167D mutants that could be eliminated by PNGase by not by EndoH, suggesting that introduction of these mutations leads to the aberrant persistence of a glycosylated 100kDa SLC4A11 species (Fig 3D and 3E).

Investigating the localization pattern of SLC4A11 mutants

Finally, we examined the possible consequences of each of the seven mutant alleles on protein localization by expressing wt or mutant in HEK293T cells followed by double immunolabeling for the HA-tagged proteins and diamidino-2-phenylindole (DAPI), a marker for DNA (Fig. 4). Once again, consistent with previous observations, we found wt SLC4A11 to localize predominantly to the plasma membrane (Fig. 4). Three mutants (p.Y526C, p.V575M and p.G834S) that processed similar to the wt SLC4A11 on immunoblot analyses likewise appeared to localize predominantly to the plasma membrane (Fig. 4; Table 1). In contrast, the other four mutants (p.E167D, p.R282P, p.G583D and p.G742R) showed a diffuse distribution in the cytoplasm (Fig. 4; Table 1).

Discussion

Here, we report data implicating heterozygous *SLC4A11* in the pathogenesis of adult-onset FCD. Sequencing of 192 unrelated FCD patients revealed seven candidate mutations. Genetic data were strongly suggestive of a pathogenic potential for each of these alleles, since none of them were present in controls; this represents a significant enrichment (Fisher's exact test 0.014). The availability of familial segregation for one of the mutant alleles in a three-generational family also supports an autosomal dominant causality model for at least one of the seven alleles, G742R, providing the first familial evidence for *SLC4A11* being a *bona fide* adult-onset FCD gene. Further functional studies provide diverse lines of evidence that each of these alleles interferes with protein function. Four of the seven alleles (p. E167D, p. R282P, p. G583D and p. G742R), when tested in a heterologous cell-based assay revealed defects in maturation, possibly due to a combination of trapping in the ER and degradation of mutant protein, while the other three alleles (p. Y526C, p. V575M and p. G834S) exhibit partial loss of localization at the membrane. While we are cautious in interpreting these data because of the *in vitro* nature of these assays, we observed complete consistency of our results when combining all lines of evidence (Table

1). Based on the combination of our genetic and biochemical analysis, our conservative estimate is that *SLC4A11* can potentially explain some 2% of the disorder in northern Europeans (4/192 patients), although larger cohorts will have to be screened to obtain more accurate estimastes.

Our data confirm and extend the recent observations by Vithana and colleagues, where they found four likely pathogenic mutations in 86 sporadic FCD patients (Vithana et al., 2008). Interestingly, we have shown previously a significant reduction of *SLC4A11* expression levels in FCD patients (Gottsch et al., 2003), suggesting either the additional presence of promoter mutations in FCD patients or that upstream loci that regulate *SLC4A11* expression might also be candidates for this disorder. Moreover, the causal involvement of *SLC4A11* also reinforces and extends the notion that the corneal endothelial dystrophies represent a phenotypic continuum with significant genetic overlap, despite their discrete clinical manifestation. We have shown recently that adult-onset FCD and juvenile-onset PPCD are allelic, by virtue of the presence of heterozygous *TCF8* missense mutations in FCD patients (Riazuddin et al., 2010); haploinsufficiency at that locus causes PPCD, since all known PPCD mutations lead to null alleles (Krafchak et al., 2005; Aldave et al., 2007), whereas residual protein activity gives rise to a later-onset disorder, FCD. A similar model can be proposed for the observed CHED-FCD relationship, where biallelic *SLC4A11* mutations give rise to the congenital disorder, whereas partial loss of function (haploinsufficiency) causes the same molecular problems but is of late onset. This is not a new paradigm in human and medical genetics: biallelic mutations in *ABCA4* cause early onset recessive retinitis pigmentosa, whereas heterozygous mutations are associated with age-related macular degeneration (Rozet et al., 1999; Allikmets et al., 1997). We cannot formally exclude the possibility that the FCD-associated mutations are dominant negative or gain of function alleles; indeed, appropriate engineering in the mouse or other model organisms would be required to address these possibilities directly. However, we favor a loss-of-function model, based on the observed failure of mutant SLC4A11 to mature and to be exported in its physiologically relevant position in the membrane. This model raises some interesting possibilities. For example, hearing function is not typically associated with FCD clinical analysis. However, the involvement of *SLC4A11* in Harboyan syndrome (Desir et al., 2007) suggests that some FCD patients might also exhibit neurosensory hearing loss that might have been erroneously attributed to natural ageing but which may, in fact, be a consequence of a mutation in *SLC4A11* or its associated pathway(s). Finally, we speculate that the identification of additional loci for any endothelial corneal dystrophy has the potential to inform the genetic architecture of all other allied clinical phenotypes through the contribution of both causal and modifying alleles; at the same time, this overlapping genetic continuum also suggests that therapeutic paradigms developed for one of the corneal dystrophies might also be beneficial across the disorder spectrum, which could be particularly important given the relative rarity of CHED and PPCD.

Acknowledgments

We thank the family members for their enthusiastic and continued participation in this study. This project was supported in part by National Eye Institute Grants R01EY016835 (JDG), the Kwok Research Fund (JDG), and the National Institute of Child Health and Development Grant R01HD04260 (NK). This work is also supported by a research grant from the BioMedical Research Council (BMRC; 07/1/35/19/520) to EN Vithana and L.-F. Seet is supported by a research grant from the SingHealth Foundation (SHF/PD002/2006). NK is a Distinguished George W. Brumley Professor.

References

Aldave AJ, Yellore VS, Yu F, Bourla N, Sonmez B, Salem AK, Rayner SA, Sampat KM, Krafchak CM, Richards JE. Posterior polymorphous corneal dystrophy is associated with TCF8 gene

mutations and abdominal hernia. Am J Med Genet A. 2007; 143A:2549–2556. [PubMed: 17935237]

Allikmets R, Shroyer NF, Singh N, Seddon JM, Lewis RA, Bernstein PS, Peiffer A, Zabriskie NA, Li Y, Hutchinson A, Dean M, Lupski JR, Leppert M. Mutation of the Stargardt disease gene (ABCR) in age-related macular degeneration. Science. 1997; 277:1805–1807. [PubMed: 9295268]

Bisceglia L, Ciaschetti M, De BP, Campo PA, Pizzicoli C, Scala C, Grifa M, Ciavarella P, Delle NN, Vaira F, Macaluso C, Zelante L. VSX1 mutational analysis in a series of Italian patients affected by keratoconus: detection of a novel mutation. Invest Ophthalmol Vis Sci. 2005; 46:39–45. [PubMed: 15623752]

Biswas S, Munier FL, Yardley J, Hart-Holden N, Perveen R, Cousin P, Sutphin JE, Noble B, Batterbury M, Kielty C, Hackett A, Bonshek R, Ridgway A, McLeod D, Sheffield VC, Stone EM, Schorderet DF, Black GC. Missense mutations in COL8A2, the gene encoding the alpha2 chain of type VIII collagen, cause two forms of corneal endothelial dystrophy. Hum Mol Genet. 2001; 10:2415–2423. [PubMed: 11689488]

Desir J, Moya G, Reish O, Van RN, Deconinck H, David KL, Meire FM, Abramowicz MJ. Borate transporter SLC4A11 mutations cause both Harboyan syndrome and non-syndromic corneal endothelial dystrophy. J Med Genet. 2007; 44:322–326. [PubMed: 17220209]

Fuchs E. Dystrophia epithelialis corneae. Graefes Arch Clin Exp Ophthalmol. 1910:478–508.

Gottsch JD, Bowers AL, Margulies EH, Seitzman GD, Kim SW, Saha S, Jun AS, Stark WJ, Liu SH. Serial analysis of gene expression in the corneal endothelium of Fuchs' dystrophy. Invest Ophthalmol Vis Sci. 2003; 44:594–599. [PubMed: 12556388]

Gottsch JD, Zhang C, Sundin OH, Bell WR, Stark WJ, Green WR. Fuchs corneal dystrophy: aberrant collagen distribution in an L450W mutant of the COL8A2 gene. Invest Ophthalmol Vis Sci. 2005; 46:4504–4511. [PubMed: 16303941]

Heon E, Greenberg A, Kopp KK, Rootman D, Vincent AL, Billingsley G, Priston M, Dorval KM, Chow RL, McInnes RR, Heathcote G, Westall C, Sutphin JE, Semina E, Bremner R, Stone EM. VSX1: a gene for posterior polymorphous dystrophy and keratoconus. Hum Mol Genet. 2002; 11:1029–1036. [PubMed: 11978762]

Hogan MJ, Wood I, Fine M. Fuchs' endothelial dystrophy of the cornea. 29th Sanford Gifford Memorial lecture. Am J Ophthalmol. 1974; 78:363–383. [PubMed: 4547212]

Klintworth GK. Corneal dystrophies. Orphanet J Rare Dis. 2009; 4:7. [PubMed: 19236704]

Krachmer JH, Purcell JJ Jr, Young CW, Bucher KD. Corneal endothelial dystrophy. A study of 64 families. Arch Ophthalmol. 1978; 96:2036–2039. [PubMed: 309758]

Krafchak CM, Pawar H, Moroi SE, Sugar A, Lichter PR, Mackey DA, Mian S, Nairus T, Elner V, Schteingart MT, Downs CA, Kijek TG, Johnson JM, Trager EH, Rozsa FW, Mandal MN, Epstein MP, Vollrath D, Ayyagari R, Boehnke M, Richards JE. Mutations in TCF8 cause posterior polymorphous corneal dystrophy and ectopic expression of COL4A3 by corneal endothelial cells. Am J Hum Genet. 2005; 77:694–708. [PubMed: 16252232]

Riazuddin SA, Eghrari AO, Al-Saif A, Davey L, Meadows DN, Katsanis N, Gottsch JD. Linkage of a mild late-onset phenotype of Fuchs corneal dystrophy to a novel locus at 5q33.1-q35.2. Invest Ophthalmol Vis Sci. 2009; 50:5667–5671. [PubMed: 19608540]

Riazuddin SA, Zaghloul NA, Al-Saif A, Davey L, Diplas BH, Meadows DN, Eghrari AO, Minear MA, Li YJ, Klintworth GK, Afshari N, Gregory SG, Gottsch JD, Katsanis N. Missense mutations in TCF8 cause late-onset Fuchs corneal dystrophy and interact with FCD4 on chromosome 9p. Am J Hum Genet. 2010; 86:45–53. [PubMed: 20036349]

Rozet JM, Gerber S, Ghazi I, Perrault I, Ducroq D, Souied E, Cabot A, Dufier JL, Munnich A, Kaplan J. Mutations of the retinal specific ATP binding transporter gene (ABCR) in a single family segregating both autosomal recessive retinitis pigmentosa RP19 and Stargardt disease: evidence of clinical heterogeneity at this locus. J Med Genet. 1999; 36:447–451. [PubMed: 10874631]

Sundin OH, Broman KW, Chang HH, Vito EC, Stark WJ, Gottsch JD. A common locus for late-onset Fuchs corneal dystrophy maps to 18q21.2-q21.32. Invest Ophthalmol Vis Sci. 2006a; 47:3919–3926. [PubMed: 16936105]

Sundin OH, Jun AS, Broman KW, Liu SH, Sheehan SE, Vito EC, Stark WJ, Gottsch JD. Linkage of late-onset Fuchs corneal dystrophy to a novel locus at 13pTel-13q12.13. Invest Ophthalmol Vis Sci. 2006b; 47:140–145. [PubMed: 16384955]

Vincent AL, Rootman D, Munier FL, Heon E. A molecular perspective on corneal dystrophies. Dev Ophthalmol. 2003; 37:50–66. [PubMed: 12876829]

Vithana EN, Morgan P, Sundaresan P, Ebenezer ND, Tan DT, Mohamed MD, Anand S, Khine KO, Venkataraman D, Yong VH, Salto-Tellez M, Venkatraman A, Guo K, Hemadevi B, Srinivasan M, Prajna V, Khine M, Casey JR, Inglehearn CF, Aung T. Mutations in sodium-borate cotransporter SLC4A11 cause recessive congenital hereditary endothelial dystrophy (CHED2). Nat Genet. 2006; 38:755–757. [PubMed: 16767101]

Vithana EN, Morgan PE, Ramprasad V, Tan DT, Yong VH, Venkataraman D, Venkatraman A, Yam GH, Nagasamy S, Law RW, Rajagopal R, Pang CP, Kumaramanickevel G, Casey JR, Aung T. SLC4A11 mutations in Fuchs endothelial corneal dystrophy. Hum Mol Genet. 2008; 17:656–666. [PubMed: 18024964]

Vogt A. Weitere Ergebnisse der Spaltlampenmikroskopie des vordern Bulbusabschnittes. Arch Ophthalmol. 1921:63–113.

Wilson SE, Bourne WM. Fuchs' dystrophy. Cornea. 1988; 7:2–18. [PubMed: 3280235]

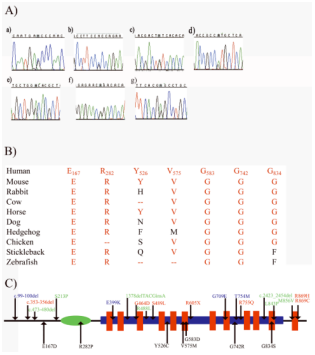

Figure 1.

A) Sequence chromatograms of the heterozygous changes identified in our cohort. a) c. 501G>C, b) c.845G>C, c) c.1577A>G, d) c.1723G>A, e) c.1748G>A and f) c.2224G>A, and g) c.2500G>A. Note: The numbering system used for sequence variations is based on cDNA sequence with +1 corresponding to the A of the ATG translation initiation codon in the GenBank Reference Sequence: NM_032034.3. **B)** Conservation of amino acid residues, identified in our patients; and **C)** A schematic illustration of the domain structure of *SLC4A11* predicted by simple modular architecture research tools (SMART) algorithms and distribution of mutations associated with different corneal endothelial dystrophies. The green oval represents the anion exchange domain, whereas the blue rectangle symbolizes the bi-carbonate domain and the transmembrane regions are denoted with red bars. Mutations implicated in CHED (red), CEPD (green), late-onset FCD identified previously (blue) and late-onset FCD identified in our cohort (black).

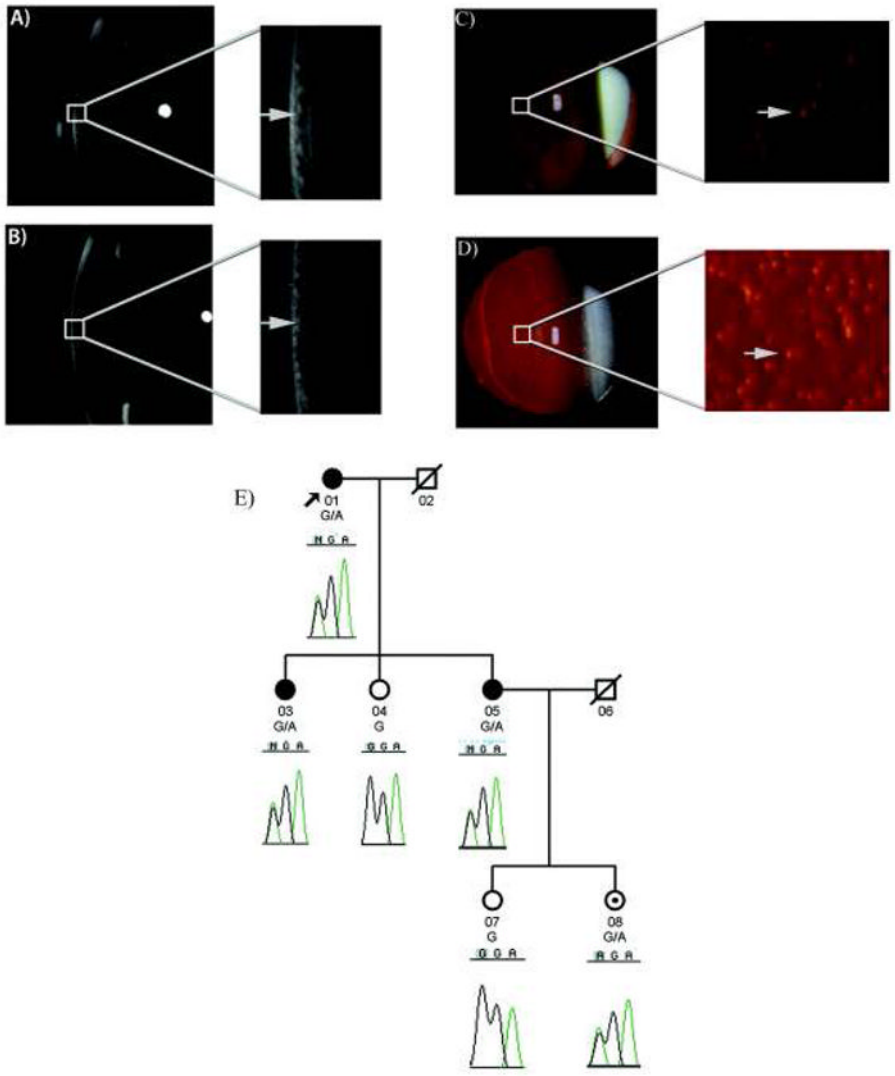

Figure 2.

Slit lamp biomicroscopy and retroillumination photographs of affected individuals of family "WO". **A & C**) individual 01, **B & D** individual 03. The image in the box is magnified on the right side. The arrow points to the guttae present in the cornea. **E)** Sequence analysis illustrating the segregation of pathogenic mutation, c.2224G>A. SLC4A11 harbors a glycine (GGA) at position 742; the G>A transition results in a glycine to arginine (AGA) substitution. Squares: males; circles: females; filled symbols: affected individuals; symbol with a dot in the middle: individual(s) with traces bilaterally, and diagonal line through a symbol: a deceased family member.

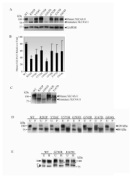

Figure 3.

Electrophoretic mobility, abundance and glycosylation of WT and mutant SLC4A11. (**A**) Immunoblot probed for SLC4A11 (HA-tag) and GAPDH resolved by 7.5% SDS-PAGE. Positions of the 120 kDa (mature) and 80 kDa (immature) forms of SLC4A11 are indicated (arrows). (**B**) Quantification of mature versus total SLC4A11 and its mutants by densitometry. The ratio of mature versus total SLC4A11 was calculated as the density of the mature 120 kDa specie over the mature 120 kDa + 80 kDa protein species × 100%. **P*<0.005, relative to WT SLC4A11 (n=3). (**C**) Immunoblot of WT and selected mutants resolved by 5% SDS-PAGE. Asterisks indicate the ~100kDa protein specie present prominently in G742R and E167D SLC4A11 mutants. **D)** Treatment of WT and mutant SLC4A11 with PNGase F (F). Cell lysates, corresponding to untreated (U) and treated with PNGase F (F), were subjected to SDS-PAGE and Western blotted with anti-HA antibody. Equal amounts of protein were loaded in each lane. Asterisks indicate the ~100kDa protein specie present in G742R and E167D that shifted on treatment with PNGase F. **E**) Treatment of WT, G742R and E167D SLC4A11 with Endo H (H). The ~100kDa protein specie present in G742R and E167D did not shift on treatment with Endo H. Migration positions of protein species were assigned as mature glycosylated (M), core glycosylated (C) and unglycosylated (N).

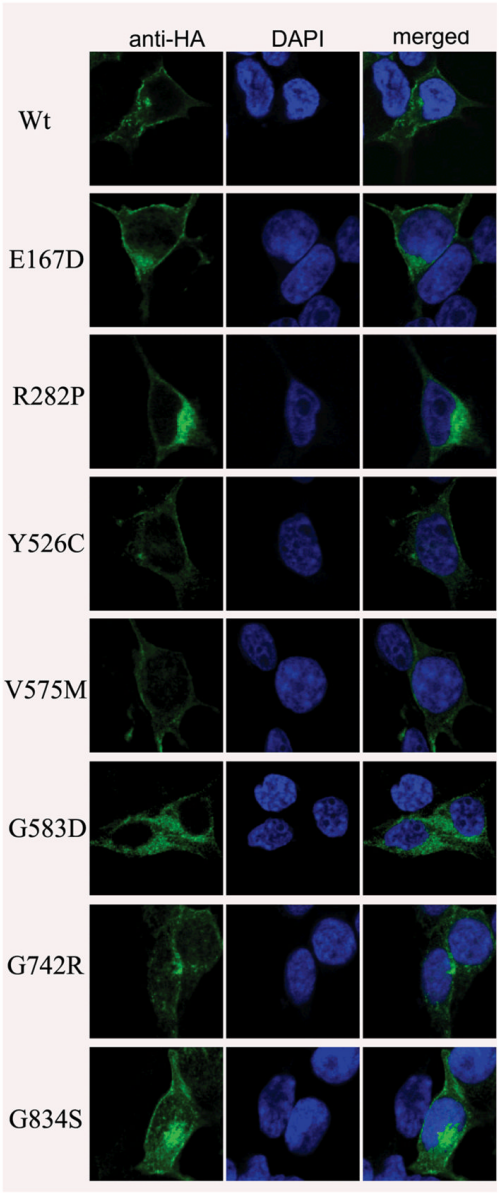

Figure 4.

Examining the localization of profile of WT and mutant SLC4A11 in HEK293T cells. HEK293T cells were transiently transfected with plasmid bearing HA-tagged WT and mutant *SLC4A11* and cells were probed with mouse monoclonal anti-HA antibody, followed by goat anti-mouse IgG conjugated to AlexaFluor 488. The nuclei were stained with 4′, 6-diamidino-2-phenylindole (DAPI).

Table 1

Genetic and biochemical characteristics of late-onset FCD mutants

No	Mutation (DNA)	Mutation (Protein)	Evolutionary conservation in *SLC4A11* orthologs	Presence in ethnically matched chromosomes	Expression and post translational modification of SLC4A11 mutants	Cellular localization
1	c.501G>C	p.E167D	H, M, R, C, Hr, D, Hd, Ch, S, Z	0 in 186	reduction in the mature 120kDa form, with addition of 100kDa species	cytoplasmic
2	c.845G>C	p.R282P	H, M, R, C, Hr, D, Hd, S, Z	0 in 186	immature form as the predominant species	cytoplasmic
3	c.1577A>G	p.Y526C	H, M, Hr	0 in 184	indistinguishable from wt	Membrane/some cytoplasmic fraction
4	c.1723G>A	p.V575M	H, M, R, C, Hr, D, Ch, S	0 in 186	indistinguishable from wt	Membrane/some cytoplasmic fraction
5	c.1748G>A	p.G583D	H, M, R, C, Hr, D, Hd, Ch, S, Z	0 in 184	immature form as the predominant species	cytoplasmic
6	c.2224G>A	p.G742R	H, M, R, C, Hr, D, Hd, Ch, S, Z	0 in 186*	reduction in the mature 120kDa form, with addition of 100kDa species	Membrane/some cytoplasmic fraction
7	c.2500G>A	p.G834S	H, M, R, C, Hr, D, Hd, Ch,	0 in 182	indistinguishable from wt	Membrane/some cytoplasmic fraction

H: human; M: mouse; R: rabbit; C: cow; Hr: horse; D: dog; Hd: hedgehog; Ch: chicken; S: stickleback; Z: zebra fish.

* represent the mutation segregating in family “WO”.

Note: The numbering system used for sequence variations is based on cDNA sequence with +1 corresponding to the A of the ATG translation initiation codon in the GenBank Reference Sequence: NM_032034.3, www.hgvs.org/mutnomen.